Iraqi Journal of Physics, 2026
https://doi.org/10.30723/ijp.v24i2.1403

Vol. 24, No.2, PP.39-49
P-ISSN: 2070-4003
E-ISSN: 2664-5548

Comparison Assessment of Synthesis and Characterization of Zr-MOFs Nanoscale Using Various Techniques

Huda J. Mohammed[1] and Samara J. Mohammad[1*]

[1]*Department of Physics, College of Science for Women, University of Baghdad, Baghdad, Iraq*
[*]Corresponding author: samaraj_phys@csw.uobaghdad.edu.iq

Abstract

Metal-Organic Frameworks (MOFs) are essential in nanotechnology applications due to their unique properties. MOFs can be easily tailored for specific uses by altering the metals or organic linkers involved, such as zirconium-based metal-organic frameworks (Zr-MOFs). Among the several methods used to create nanoscale Zr-MOFs are microwave-assisted synthesis, solvothermal, sonochemical, ionothermal, and mechanochemical procedures. The synthesis, structure, and characterization of Zr-MOFs were compared in this project between conventional solvothermal and microwave-assisted methods for nitrogen adsorption/desorption. Using X-ray diffraction (XRD) analysis, Fourier transform infrared spectroscopy (FTIR), and thermogravimetric analysis (TGA), the two processes for synthesizing Zr-MOFs were characterized. The outcomes demonstrate the crystalline structure of both MOFs. The key benefits of microwave-assisted synthesis over other methods are its quick nucleation rate, short reaction time, and improved Zr-MOF characteristics. Furthermore, the microwave-assisted method significantly accelerated the synthesis process, achieving complete reaction within 10 minutes at 120 °C, whereas the conventional process typically takes 24 hrs. The results revealed that nitrogen adsorption/desorption by Zr-MOF microwave-assisted synthesis is more dominant than the conventional solvothermal synthesis technique.

Article Info.

Keywords:
Metal–Organic Framework (MOF), Porous Materials, Microwave -Assisted Synthesis, Solvothermal Synthesis, N_2 Adsorption.

Article history:
Received: Nov. 23, 2024
Revised: May, 09, 2025
Accepted:May, 26, 2025
Published:Jun. 01,2026

1. Introduction

As an emerging class of highly ordered crystalline porous materials, Metal-Organic Frameworks (MOFs) with various potential applications have become a new research hotspot in chemistry and materials science during the last few decades, which is mainly attributed to their exceptionally high surface area, tunable pores, as well as intriguing functionalities [1]. Many studies have demonstrated that MOFs perform excellently in various applications compared to traditional porous solid materials, such as zeolites and carbon-based porous materials. Much effort has been devoted to constructing MOFs with improved stability [2]. Zirconium-based metal-organic frameworks (Zr-MOF) are among the most promising of the many MOFs because of their high stability, porosity, and distinctive de-hydroxylation activity, as widely reported in the literature [3, 4]. Because of the tight link between Zr-carboxylate and Zr-MOF, Zr-MOF has attracted a lot of interest for its extraordinarily high chemical and thermal stability [5]; this has made it possible to employ Zr-MOF in environmental applications in a new way. Additionally, Zr-MOF material can be synthesized using a microwave-assisted heating technique, which significantly reduces the synthesis time compared to other techniques [6].

Nanoscale MOFs preserve the unique chemistry and porosity of MOFs while unlocking new capabilities due to their small size, including in biomedicine, catalysis, and advanced materials. This is largely due to the exceptional area of the surface for MOFs, adjustable pore sizes, and versatile chemical processes [7]. In contrast to conventional porous substances that are solid, such as bentonite made of carbon and zeolites nanopowder porous materials [8], MOFs have been shown in numerous studies to perform exceptionally well in a variety of applications, including energy storage, separation, catalysis, chemical sensing, and drug delivery [9]. The majority of these findings, nonetheless, are thought to be conceptual because the materials' applicability is not guaranteed by perfect performances or a lack of economic evaluation. Metal-organic frameworks

are created through the coordination bonding of metal ions and organic ligands, in contrast to many industrially used materials that have homogeneous covalent connections. In most research domains, due to the reversible nature of coordination bonds, MOFs' inadequate stability is the primary barrier to their practical usage [10]. It is difficult for researchers to successfully synthesize MOFs since they must modify the synthesis conditions to produce amounts appropriate for practical uses. Thus far, solvothermal synthesis has been the predominant technique used to create MOFs, requiring a large energy input and a long reaction time [11]. For this reason, the scientific community is very interested in developing more affordable and sustainable synthetic methods.

Microwave-assisted synthesis has gained popularity as an alternate technique for both organic and inorganic materials due to its ability to shorten the time needed to synthesise porous materials, like MOFs, from days to minutes [12]. Because of the microwave's quicker rate of nucleation, the crystallization process for the creation of porous materials is sped up. Using a microwave to help synthesis, it is possible to avoid using the various very toxic solvents needed for conventional MOF synthesis. Further evidence of the approach's significance for future endeavors comes from the considerable improvements in the properties and functionality of MOFs made via microwave synthesis [13]. Instead of conducting heat to the media from outside heating sources, as with conventional heating, microwave synthesis generates heat internally within the reaction media by dielectric heating [14]. Therefore, it is possible to start a consistent, high-temperature heating process under microwave radiation, which will help with MOF synthesis by promoting crystal nucleation and growth [15]. The microwave-assisted synthesis has established itself as a key player in the synthesis of MOFs. The shortened reaction time, rapid nucleation rate, and altered MOF characteristics are the primary benefits of microwave-assisted synthesis. One of the main benefits of microwave irradiation is that it heats the sample uniformly throughout, eliminating the need for heat transmission within the mixture. The scaling-up process is less difficult since the reaction mixture's volume is not reliant on the heating process [16].

In this study, Zr-MOFs were synthesized using two different approaches: conventional solvothermal and microwave-assisted methods. Then, the synthesis techniques were compared to evaluate their influence on nitrogen adsorption behavior in Zr-MOFs. X-ray diffraction (XRD) analysis, Fourier transformed infrared spectroscopy (FTIR), thermogravimetric analysis (TGA), and Brunauer, Emmet, and Teller (BET) surface area analysis were used to characterize the produced MOFs.

The goal of the study is to compare two synthesis methods (solvothermal and microwave-assisted) of Zr-MOFs at the nanoscale and determine which approach produces the best results. Comparing synthesis techniques makes it easier to find economical and ecologically friendly production paths that work well for large-scale operations. Furthermore, the purpose of this project is to assist sustainable development goals by examining low-energy or solvent-free synthesis approaches consistent with green chemistry principles.

2. Materials and Methods

2.1 Raw Materials

The analytical-grade materials and reagents used in this experiment comprised zirconium oxychloride octahydrate (98% $ZrOCl_2.8H_2O$, Glentham Life Sciences, Germany), terephthalic acid (BDC, 97%, Sigma Aldrich USA), N, N-dimethylformamide (DMF, 99.9%, SDFCL GROUP India, methanol (99.9%, Sydney Solvents, Australia), 1,3,5-benzenetricarboxylic acid (98%, Sigma Aldrich USA), and deionized water. All compounds were utilized exactly as they were supplied without additional purification. Table 1 lists all the chemicals used in this research.

Table 1: List of chemicals used in this project.

Name of chemicals	Formula	Company Name	Purity
zirconium oxychloride octahydrate	Cl_2OZr8H_2O	Glentham Life Sciences Germany	98%
Terephthalic acid (BDC)	$C_8H_6O_4$	Sigma Aldrich, USA	97%
1,3,5-benzenetricarboxylic acid	$C_9H_6O_6$	Sigma Aldrich, USA	98%
N, N-dimethylformamide (DMF)	C_3H_7NO	SDFCL GROUP, India	99.9%
Deionized water		Aqua Science, USA	Ultrapure
Methanol	CH_3OH	Sydney Solvents, Australia	99.9%

2.2. Synthesis Techniques

2.2.1. Conventional Solvothermal Synthesis

The MOFs employed in this method were typically created by heating them in an oven using a solvent different than water or by employing solvothermal methodology, as per previous studies [17]. The solvothermal approach was chosen with consideration for the starting material's solubility. Various solvothermal solvents, including methanol and dimethylformamide (DMF), are employed, contingent upon the central metal and linker utilized. The Zr-MOFs were made using the solvothermal oven heating technique. 75 mg of $ZrOCl_2$ was dispersed in 5 mL of DMF and sonicated for 10 minutes. A simultaneous reaction involved dissolving 1.25 g of 1,3,5-benzenetricarboxylic acid in 5 mL of DMF and sonicating it for 10 minutes. The two solutions were mixed in a glass vial and heated at 120 °C for 24 hrs to get Zr-MOFs. The Zr-MOF was centrifuged for 15 minutes. The resulting white precipitate was washed three times using methanol as a solvent.

To reduced structural defects and strain size For MOFs, the annealing process is essential to the synthesis of pure nanoparticles free of water molecules since the annealing temperature enhances crystal size and improves crystallinity [18]. Therefore, the sample was annealed in a furnace (Model number: TA2-16-14TP, China) at an annealing temperature of 100 ℃ for 2 hrs, and this can remove or modify surface ligands or adsorbates, tailoring the surface for specific applications (e.g., sensors or drug delivery).

2.2.2. Microwave-Assisted Synthesis

The usage of microwave radiation has expanded greatly in recent years. This has to do with how environmentally friendly it is. In this case, the moving charge of the solvent interacts with the electromagnetic field. More specifically, the applied electric field is related to the constant dipole moment of the molecule, which causes the liquid mixture to heat up quickly [19]. This process transforms electromagnetic energy into thermal energy. The microwave-assisted synthesis is similar to the solvothermal synthesis (oven heating procedure), but with a few slight adjustments. 75 mg of $ZrOCl_2$ was dispersed in 5 mL of DMF and sonicated for 10 minutes. A simultaneous reaction involved dissolving 1.25 g of 1,3,5-benzenetricarboxylic acid in 5 mL of DMF and sonicating it for 10 minutes. The two solutions were mixed in a glass vial and heated at power (228 W\s ~ 120 °C) for (10 min.) in the microwave; this resulted in a white precipitate, which was washed in DMF and methanol to exchange solvents and get rid of any remaining impurities and unreacted metals from the framework's pores. This was followed by centrifugation at 2000 rpm for 15 min. The Zr-MOF was produced as a solid substance.

3. Results and Discussion

3.1. Zr-MOF Characterization

3.1.1. XRD Characterization

A nondestructive analysis method used in solid-state chemistry is powder X-ray diffraction (XRD) to determine the structures of crystals and characterize them based on their unique diffraction patterns [20]. Fig. 1 shows diffraction patterns of the synthesised Zr-MOFs using the two synthesis methods. The data was collected using a powder X-ray diffractometer (XRD, Philips Analytical, PW1835) that is outfitted with a Cu anode radiation source (λ = 1.5406 Å) in a Bragg angle 2θ ranging from 5° to 60°. The scanning speed was set to 5 deg/min, with a step size of 0.05°. It was used for both synthesis methods to ascertain the phase identity, crystallinity, and structural features of Zr-MOFs.

The XRD patterns indicated that the synthesised Zr-MOFs' most likely diffraction peaks were located below a scattering angle (2θ) of 10 degrees, indicating that the MOF agrees with previous studies [21, 22]. Intensive peaks appearing at small 2θ angles are characteristics of porous materials, which possess abundant pores or cavities, and this appeared clearly for the two Zr-MOF XRD patterns (the microwave-assisted synthesis and the solvothermal synthesis). The possible reason for this could be the inverse relationship between 2θ and the adsorbent's porosity. The major peaks observed with high intensity were at 2θ of 6.85°, 8.25°, 12.2°, 17.35°, 21.5°, 25.6° and 35.15° indexed to the crystal planes 111, 002, 022, 004, 115, 224 and 046, respectively. This revealed the MOF crystal structure to be a symmetric cubic with strong crystallinity and the creation of massive crystals, which aligned with the distinctive diffraction pattern of the Zr MOF phase structure [23, 24].

The average crystallite size of the Zr MOF for both syntheses was calculated according to the Debye Scherrer formula, using Eq. (1):

$$D = \frac{k\lambda}{\beta \cos\theta} \quad (1)$$

where D is the crystallite size, λ is the wavelength of the radiation, k is the geometric factor, β is the full width at half maximum (FWHM).

The obtained results of the crystal size by the microwave-assisted synthesis produced Zr-MOF nanoparticles only after 10 minutes of reaction time, whereas the conventional solvothermal synthesis required 24 hours to produce high-quality crystals, as shown in Table 2. However, it was noted from the results that both methods produced nanoparticles in similar small proportions.

The highest peak intensity, indexed to the (111) crystal plane at 6.85°, was selected for calculations because it appears clearly in the blue pattern corresponding to Zr-MOF synthesized via oven heating. A lower-intensity peak at the same angle (6.85°) with a FWHM of 0.198 was observed in the red pattern, representing Zr-MOF synthesized via microwave-assisted methods. This observation aligns well with previously reported XRD spectra for Zr-MOFs [21].

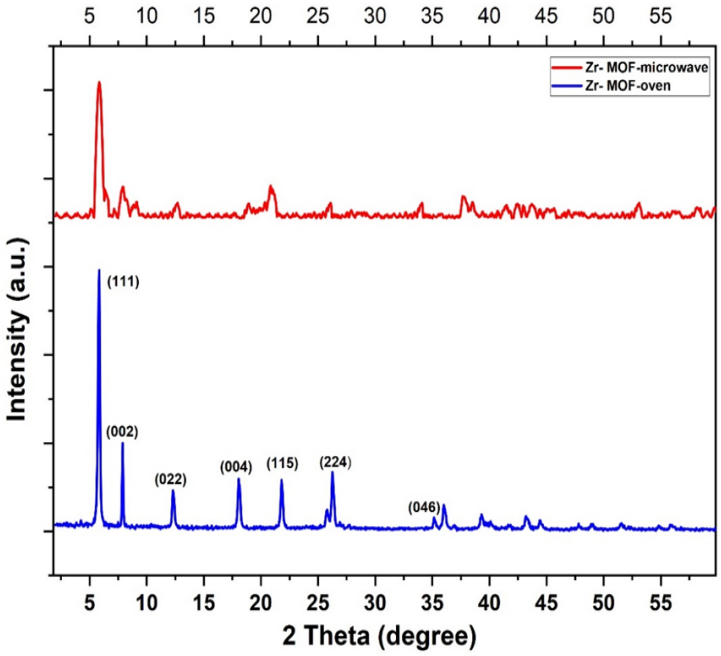

Figure 1: XRD patterns of Zr-MOFs obtained with different synthesis methods.

Table 2: Structural properties of the synthesised Zr-MOFs for both synthesis methods.

Synthesis method	Reaction time	Morphology of Zr-MOF crystals	FWHM	d-spacing (nm)	Crystal size (nm)
solvothermal	24 h	Octahedral	0.272	3.57	61.37
Assisted-microwave	10 min.	Cubic	0.198	4.38	87.63

3.1.2. FTIR Spectrum

The functional groups on pore surfaces can be investigated using the FTIS [25], which is also useful for characterizing functionalized MOFs, assessing their potential uses, and assessing the activation process. Fig. 2 illustrates the FTIR spectra of Zr-MOFs synthesised by the two methods, which can be used to identify the distinctive vibrational peaks that are symmetrical and asymmetrical. The MOF structure's O-H bond stretching is the reason for the peak at wavenumber 3415cm^{-1}. The ligand BDC possesses two carboxylate groups that are strongly coupled. These groups result in two distinct peaks: a symmetric C-O stretching band at 1396 cm^{-1} and an asymmetric C-O stretching band at 1618 cm^{-1}. These peaks might possibly be indicative of the metal's coordination bonding to the organic portion of terephthalic acid [26]. Moreover, the structure's ligand's C=C benzene ring could be the source of the tiny bands at 1504 cm^{-1} [27].

It is possible to see various peaks with low intensities; the Zr–(OC) asymmetric stretch is represented by the band around 553 cm^{-1}, and the μ3-O and μ3-OH stretches are represented by the bands around 640 and 775 cm^{-1}, respectively [28]. When Zr-MOF is synthesised using the microwave-assisted method, the OH peak at 3415 cm^{-1}, and the C-O group at peaks 1618 and 1396 cm^{-1} become more prominent, revealing the difference between the two spectra. Both Zr-MOF synthesis approaches produced FTIR spectra that closely match those found in earlier research, confirming the successful formation of the expected functional groups [29-31].

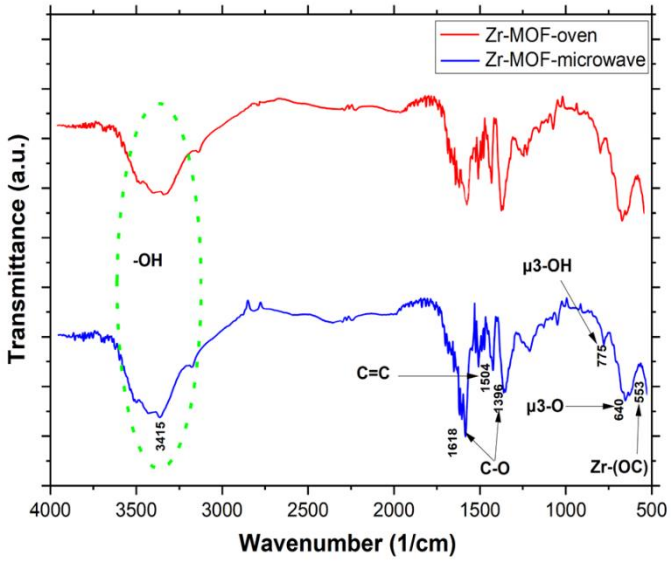

Figure 2: FTIR spectra of Zr-MOFs synthesised by the two methods (solvothermal and microwave-assisted method).

3.1.3. ThermoGravimetric Analysis (TGA)

TGA involves adjusting the weighted mass based on the sample material's temperature. It can be utilized to ascertain a material's thermal stability and breakdown products since it offers a quantifiable measurement of the mass changes in a material connected to both material transitions and thermal deterioration [32]. This method was used to investigate the thermal stability of Zr-MOF.

The TGA curves of the two methods for synthesised Zr-MOF samples are shown in Fig. 3. It is evident that Zr-MOF had three stages of weight loss, with a total mass decrease of -61.24%. The first weight loss of 9.32%, observed in the temperature range of 50–200 °C, is attributed to the evaporation of surface-adsorbed water in the Zr-MOF. The breakdown of DMF is responsible for the second weight loss of 12.76%, which occurred at a temperature between 220 and 350 °C. The third stage of weight loss was 18.06% in the range (350-600 °C), corresponding to Zr-MOF breaking down into ZrO_2. By comparing the two curves for both methods, it is noted that the Zr-MOF synthesis by the microwave-assisted method exhibited less weight loss than the Zr-MOF synthesis by oven heating, specifically in the initial and third phases. The last stage begins at around and above 600 °C, which aligns with the terephthalic acid combustion and sample framework degradation reported for other MOF materials in the literature [33]. The final product formed after heating Zr-MOF to 600 °C was ZrO_2, as can be corroborated by the XRD data and prior research, and the residual weight at 800°C was 25%. These results agree with those of Makhanya et al. [34].

Ultimately, the structural robustness and thermal stability of Zr-MOFs up to 600°C with a constant mass loss of 20% and 18% for solvothermal and the microwave-assisted methods, respectively, were validated based on the results of the TGA study. When microwaves are used, the shorter reaction times can result in fewer trapped solvents or unreacted precursors, leading to a more distinct initial mass loss. As a result, Zr-MOFs produced through microwave methods tend to have impressive thermal stability, typically breaking down around 500–600 °C, as indicated by TGA. This stability is quite comparable to that of their conventionally synthesized counterparts. However, the differences in the weight loss of the samples are caused by solvent molecules in the material's pore interior and pretreatment (both hydrated and dehydrated) [35, 36].

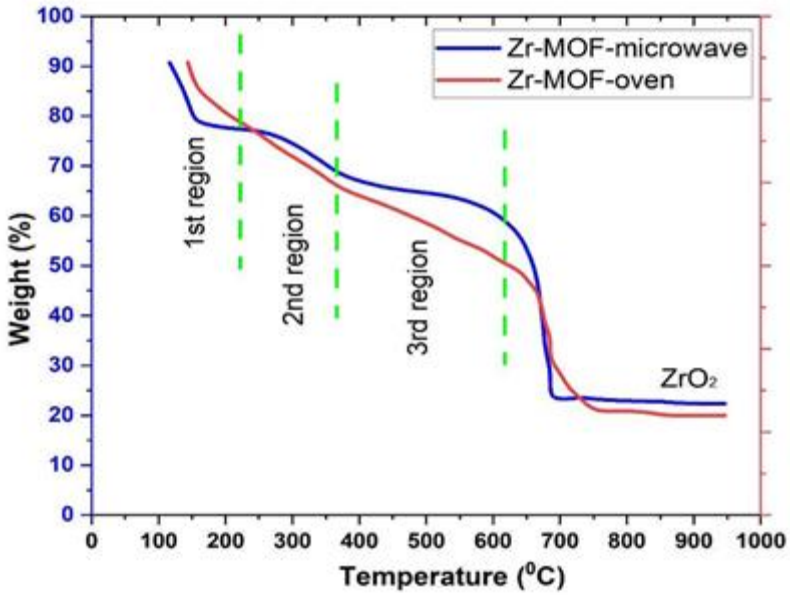

Figure 3: TGA curves of the Zr-MOFs synthesised by the microwave-assisted and the solvothermal methods at 120 °C.

3.1.4. BET Surface Area Analysis

The Brunauer, Emmet and Teller (BET) method is utilised to determine the porosity of the adsorbent by measuring the nitrogen adsorption/desorption isotherm. To investigate the porous characteristics of the Zr-MOFs samples and assess their ability for the adsorption process, the N_2 adsorption isotherms were obtained at -195 °C.

Isotherms for the Zr-MOFs samples are shown in Fig. 4 for both synthesis methods, which were prepared at 120 °C. When adsorption occurred at the extremely low pressure of P/P_0 (where P is the equilibrium pressure of adsorbate gas, and P_0 is the saturation pressure of the adsorbate gas), all adsorption isotherms demonstrated a sharp uptake, which was followed by a plateau [37]. The micropores that predominately existed in the Zr-MOFs samples were evident from these adsorption curves. Pores with a width of no more than two nanometers are called micropores. An N_2 filling of Zr-MOFs was made possible by the improved adsorbent-adsorbate Zr-MOFs and N_2 interactions caused by such a small gap. The BET equation for determining surface area is shown in its simplest form in Eq. (2):

$$S_t = Z\left(\frac{1-P}{P_\circ}\right)V_a \qquad (\mathbf{2})$$

where S_t is the sample's total surface area, Z is the nitrogen constant, P/Po is the equilibrium to saturation pressure equal to 0.294 by 30% N_2/70% He gas mixture, and V_a is the absorption's N_2 volume.

Table 3 contains the measurements of porous materials for particular locations. The results of surface area were obtained according to Eq. (2), where the as-synthesised Zr-MOFs samples had specific surface areas between 900 and 1200 m^2/g. The Zr-MOF sample synthesized by microwave had a surface area of 1210 m^2/g, and the Zr-MOF sample synthesized by the solvothermal method had a surface area of only about 945 m^2/g. For this set of samples, the N_2 adsorption isotherms were used to compute the pore diameter and micropore volume in addition to the specific surface areas. Regarding these samples, the micropore volume corresponded to their surface areas.

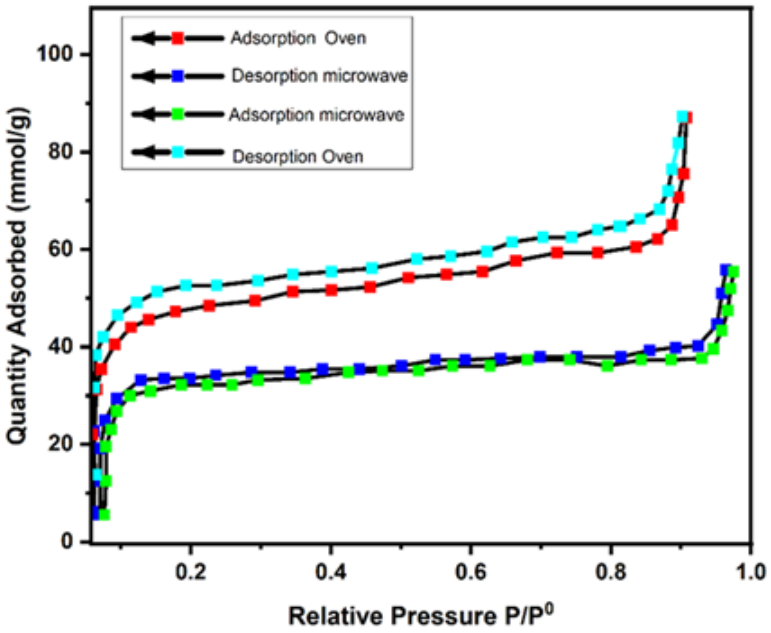

Figure 4: *N_2 adsorption/desorption isotherms for both synthesis methods with pH=6.*

Table 3: Surface characterization results for Zr-MOFs with both synthesis (solvothermal and microwave-assisted methods).

Surface area	Synthesis by oven	Synthesis by microwave
Specific surface area (BET) (m^2/g)	945	1210
Langmuir Surface Area (m^2/g)	968.3	1346.2
BJH Adsorption cumulative surface area of pores (m^2/g)	342.6	422.5
BJH Desorption cumulative surface area of pores (m^2/g)	337.9	416.3
Adsorption average pore width Å	64.1	77.3
Desorption average pore width Å	70.4	79.2
Adsorption pore volume (cm^3/g)	0.535	0.572
Desorption pore volume (cm^3/g)	0.564	0.593
Pore diameter (nm)	1.04	1.12

As shown in the adsorption/desorption isotherm diagram, the calculated values for the Zr-MOF samples align well with their microscopic features and specific surface area data measured at pH 6. As shown in Fig. 4, the formation of a hysteresis loop is visible. This narrow loop can indicate a narrow pore size distribution. Hysteresis loops are typically connected to mesopore filling and emptying, and they can be seen in the multilayer range of physisorption isotherms. For mesopore size analysis, the desorption branch was preferred for a long time, but this approach is currently deemed dubious since the desorption path might be influenced by network percolation effects [38].

4. Conclusions

In the current project, a successful synthesis of Zr-MOFs was achieved using two different methods: solvothermal and microwave-assisted. Zr-MOFs were characterized using XRD, FTIR, and TGA analysis. From characterization data, it is concluded that the synthesis method of MOFs using microwaves has faster kinetics and heating than the traditional synthesis approach. N_2

adsorption/desorption on Zr-MOF by both syntheses was studied. The adsorption of Zr-MOF via solvothermal and microwave-assisted methods was investigated, and the results from microwave synthesis were better than those from other methods. Finally, from the adsorption/desorption results of Zr-MOF for both methods, it was found that the microwave-assisted technique was better for environmental applications due to its speed, cleanliness, and safety from toxic materials.

Acknowledgements

The authors gratefully acknowledge the Iraqi Ministry of Higher Education for the financial support. Also, the authors thank the Petroleum Research and Development Center (PRDC)-Ministry of Oil in Iraq for implementing the characterization analysis.

Conflict of Interest

The authors declare that they have no conflict of interest.

References

1. M. Zaltraiov, Metal-organic frameworks: Emerging porous materials for energy applications, *Advances in Energy Material*, (Apple Academic Press, 1st Edition, 2023), **47**, P. 29. https://doi.org/10.1201/9781003346074-3.
2. M. Gatou, I. Vagena, N. Lagopati, N. Pippa, M. Gazouli, and E. Pavlatou, Functional MOF-based materials for environmental and biomedical applications: A critical review, *Nanomater.* **13**(15), 2224 (2023). https://doi.org/10.3390/nano13152224.
3. K. Chattopadhyay, M. Mandal, and D. Maita, A review on zirconium-based metal–organic frameworks: synthetic approaches and biomedical applications, *Mater. Adv.* **5**(1), 51 **(**2024). https://doi.org/10.1039/D3MA00735A.
4. A. L. Bugaev, A. A. Guda, K. A. Lomachenko, E. G. Kamyshova, M. A. Soldatov, and G. Kaur, *Operando* study of palladium nanoparticles inside UiO-67 MOF for catalytic hydrogenation of hydrocarbons, *Faraday Discuss*. **208**, 287 (2018). https://doi.org/10.1039/C7FD00224F.
5. Y. An, X. Lv, W. Jiang, L. Wang, Y. Shi, X. Hang, and H. Pang, The stability of MOFs in aqueous solutions-research progress and prospects, *Green Chem. Eng.* **5**(2), 187 **(**2024). https://doi.org/10.1016/j.gce.2023.07.004.
6. H. Liu, Y. Zhao, C. Zhou, B. Mu, and L. Chen, Microwave-assisted synthesis of Zr-based metal–organic framework (Zr-fum-fcu-MOF) for gas adsorption separation, *Chem. Phys. Lett.* **780**, 138906 (2021). https://doi.org/10.1016/j.cplett.2021.138906.
7. U. Shahzad, H. M. Marwani, M. Saeed, A. M. Asiri, R. H. Althomali, and M. M. Rahman, Exploration of porous metal-organic frameworks (MOFs) for an efficient energy storage applications, *J. Energy Storage.* **74**(A), 109518 (2023). https://doi.org/10.1016/j.est.2023.109518.
8. S. J. Mohammad, H. H. Rady, and S. S. Najim, Remove phenolic pollutant on Bentonite surface nanopowder, *In AIP Conference Proceedings*; **2437**(1), 020187 (2022). https://doi.org/10.1063/5.0094046.
9. E. Abd Dleam and S. H. Kareem, Mesoporous Silica Nanoparticles as a System for Ciprofloxacin Drug Delivery; Kinetic of Adsorption and Releasing, *Baghdad Sci. J.*, **18**(2), 0357 (2021). https://doi.org/10.21123/bsj.2021.18.2.0357.
10. X. Zhang, S. Zhang, Y. Tang, X. Huang, and H. Pang, Recent advances and challenges of metal–organic framework/graphene-based composites, *Compos. B. Eng.*, **230**, 109532 (2022). https://doi.org/10.1016/j.compositesb.2021.109532.
11. T. Azbell, T. Pitt, M. Bollmeyer, C. Cong, K. Lancaster, and P. Milner, Solvent-Free Synthesis of Metal-Organic Frameworks Using Low-Melting Metal Salts, *Mater. Chem.* **1**, (2022). https://doi.org/10.26434/chemrxiv-2022-00xd7.
12. A. K. Alwan, M. J. Kahadom, A. M. Marai, and A. K. Esmaeel, Comparison Between Conventional and Microwave Methods For Extraction Pectin and Degree of Esterification from Orange (Citrus sinesis) and Grapefruit (Citrus paradisi) Peels, *Baghdad Sci. J.*, **13**(1), 0026, (2016). https://doi.org/10.21123/bsj.2016.13.1.0026.
13. R. Krishnan, S. N. Shibu, D. Poelman, A. K. Badyal, A. K. Kunti, H. C. Swart, and S. G. Menon, Recent advances in microwave synthesis for photoluminescence and photocatalysis, *Mater. Today Commun.* **32**, 103890, (2022). http://dx.doi.org/10.1016/j.mtcomm.2022.103890.
14. N. B. Kardile, S. M. Thakre, and A. Sinha, Chapter 9 - Electric and magnetic field based processing technologies for food. *Current Developments in Biotechnology and Bioengineering, Elsevier*, 239, (2022). http://dx.doi.org/10.1016/B978-0-323-91158-0.00012-0.
15. E. Taki and D. Sami, A review on Activated Carbon Prepared from Agricultural Waste using Conventional and Microwave Activation, *Khwarizmi eng. j.* **19**(3), 33, (2023). https://doi.org/10.22153/kej.2023.06.001.

16. P. T. Phan, J. Hong, N. Tran, and T. H. Le, The properties of microwave-assisted synthesis of metal-organic frameworks and their application, *Nanomater.* **13**(2), 352, (2023). https://doi.org/10.3390/nano13020352.
17. V. F. Yusuf, N. I. Malek, and S. K. Kailasa, Review on Metal–Organic Framework Classification, Synthetic Approaches, and Influencing Factors: Applications in Energy, Drug Delivery, and Wastewater Treatment, *ACS Omega,* **7**(49), 44507 (2022). https://doi.org/10.1021/acsomega.2c05310.
18. D. K. Muthee and B. F. Dejene, Effect of annealing temperature on structural, optical, and photocatalytic properties of titanium dioxide nanoparticles, *Heliyon.* **7**(6), 6 (2021). https://doi.org/10.1016/j.heliyon.2021.e07269.
19. K. Hyjek and P. Jodłowski, Metal-organic frameworks for efficient drug adsorption and delivery, *Sci. Radices*, **2**(2), 89 (2023). https://doi.org/10.58332/scirad2023v2i2a03.
20. M. Leśko, J. Samuelsson, D. Åsberg, K. Kaczmarski, and T. Fornstedt, Evaluating the advantages of higher heat conductivity in a recently developed type of core-shell diamond stationary phase particle in UHPLC, *J. Chromatogr. A*. **1625**, 461076 (2020). https://doi.org/10.1016/j.chroma.2020.461076.
21. A. Ali, Y. W. Chiang, and R. M. Santos, X-ray diffraction techniques for mineral characterization: A review for engineers of the fundamentals, applications, and research directions, *Minerals*, **12** (2), 205 (2022). https://doi.org/10.3390/min12020205.
22. K. D. Nguyen, N. T. Vo, K. T. Le, K. V. Ho, N. T. Phan, P. H. Ho, and H. V. Le, Defect-engineered metal–organic frameworks (MOF-808) towards the improved adsorptive removal of organic dyes and chromium (VI) species from water *New J. Chem.,* **47**(11), 6433 (2023). https://doi.org/10.1039/D2NJ05693C.
23. Y. Jiang, Z. Wang, Z. Zhu, M. He, and P. Zhou, Effective removal of humic acid by Zr-MOFs with surface modification, Water. **14**(11), 1800 **(**2022). https://doi.org/10.3390/w14111800.
24. X. Zhang, R. Yu, D. Wang, W. Li, and Y. Zhang, Green Photocatalysis of Organic Pollutants by Bimetallic Zn-Zr Metal-Organic Framework Catalyst, *Front. Chem.*, **10**, 918941 **(**2022). https://doi.org/10.3389/fchem.2022.918941.
25. F. ALjubouri and M. K. Jawad, FTIR and electrical behavior of blend electrolytes based on (PVA/PVP), *Iraqi J. Phys.*, **21**(1), 1 (2023). https://doi.org/10.30723/ijp.v21i1.1093.
26. H. R. Abid, M. R. Azhar, S. Iglauer, Z. H. Rada, A. Al-Yaseri, and A. Keshavarz, Physicochemical characterization of metal organic framework materials: A mini review, *Heliyon*, **10**(1), e23840 **(**2024). https://doi.org/10.1016/j.heliyon.2023.e23840.
27. S. Li, X. Hu, Q. Chen, X. Zhang, H. Chai, and Y. Huang, Introducing bifunctional metal-organic frameworks to the construction of a novel ratiometric fluorescence sensor for screening acid phosphatase activity, *Biosens and Bioelectron*, **137**, 133 (2019). https://doi.org/10.1016/j.bios.2019.05.010.
28. M. S. Alivand, N. H. Tehrani, M. Shafiei-Alavijeh, A. Rashidi, M. Kooti, A. Pourreza, and S. Fakhraie, Synthesis of a modified HF-free MIL-101(Cr) nanoadsorbent with enhanced H_2S/CH_4, CO_2/CH_4, and CO_2/N_2 selectivity, J. *Env. Chem. Eng.*, **7**(2), 102946 (2019). https://doi.org/10.1016/j.jece.2019.102946.
29. N. Aljammal, J. Lauwaert, B. Biesemans, T. Vandevyvere, M. K. Sabbe, P. M. Heynderickx, and J. W. Thybaut, UiO-66 metal-organic frameworks as aldol condensation catalyst: Impact of defects, solvent, functionality on the catalytic activity and selectivity, *J. Catal.*, **433**, 115471 (2024). https://doi.org/10.1016/j.jcat.2024.115471.
30. Z. U. Zango, N. S. Sambudi, K. Jumbri, N. H. Bakar, N. A. Abdullah, E. S. Negim, and B. Saad, Experimental and molecular docking model studies for the adsorption of polycyclic aromatic hydrocarbons onto UiO-66(Zr) and NH_2-UiO-66(Zr) metal-organic frameworks, *Chem. Eng. Sci.*, **220**, 115608 (2020). https://doi.org/10.1016/j.ces.2020.115608.
31. L. Rahmidar, D. G. Syarif, Suyatman, and Nugraha, A facile approach for preparing Zr-BDC and Zr-BDC-NH_2 MOFs using solvothermal method, *In J. Phys.: Conf. Ser.*, **2243**, 012055, (2022). https://doi.org/10.1088/1742-6596/2243/1/012055.
32. T. Ma, W. Wang, and R. Wang, Thermal degradation and carbonization mechanism of Fe-based metal-organic frameworks onto flame-retardant polyethylene terephthalate, *Polymers*, **15**(1), 224, (2023). https://doi.org/10.3390/polym15010224.
33. T. Emiola-Sadiq, L. Zhang, and A. K. Dalai, Thermal and Kinetic Studies on Biomass Degradation *via* Thermogravimetric Analysis: A Combination of Model-Fitting and Model-Free Approach, *ACS Omega*, **6**(34), 22233 (2021). https://doi.org/10.1021/acsomega.1c02937.
34. N. P. Makhanya, B. Oboirien, N. Musyoka, J. Ren, and P. Ndungu, Evaluation of PET-derived metal organic frameworks (MOFs) for water adsorption and heat storage, *J. Porous Mater.* **30**, 387 (2023). https://doi.org/10.1007/s10934-022-01351-w.
35. B. Kebede, A. M. Taddesse, and E. Teju, UiO-66 (Zr-MOF): Synthesis, Characterization, and Application for the Removal of Malathion and 2, 4-D from Aqueous Solution, *Environ. Pollut. Bioavailab*, **35**(1), 2222910, (2023). https://doi.org/10.1080/26395940.2023.2222910.
36. M. Saidi, P. H. Ho, P. Yadav, F. Salles, C. Charnay, L. Girard, L. Boukli, and P. Trens, Zirconium-Based Metal Organic Frameworks for the Capture of Carbon Dioxide and Ethanol Vapour. A Comparative Study, *Molecules*, **26**, 7620 (2021). https://doi.org/10.3390/molecules26247620.

37. M. Thommes, K. Kaneko, A.V. Neimark, J. P. Olivier, F. Rodriguez, J. Rouquerol, and K. Sing, Physisorption of gases, with special reference to the evaluation of surface area and pore size distribution (IUPAC Technical Report), *Pure Appl. Chem.* **87**(9-10), 1051 **(**2015). https://doi.org/10.1515/pac-2014-1117.
38. Q. Ren, Y. Ma, F. Wei, L. Qin, H. Chen, Z. Liang, and S. Wang, Preparation of Zr-MOFs for the adsorption of doxycycline hydrochloride from wastewater, *Green Process. Synth.* **12**(1), 20228127 **(**2023). https://doi.org/10.1515/gps-2022-8127.

تقييم مقارنة لتخليق وتوصيف أطر الزركونيوم المعدنية النانوية باستخدام تقنيات مختلفة

هدى جعفر محمد[1] وسمارة جاسم محمد[1]
[1] قسم الفيزياء، كلية العلوم للبنات، جامعة بغداد، بغداد، العراق

الخلاصة
تعتبر الأطر المعدنية العضوية ضرورية في تطبيقات التكنولوجيا النانوية بسبب خصائصها الفريدة. يمكن تصميم الأطر المعدنية العضوية بسهولة لاستخدامات محددة عن طريق تغيير المعادن أو الروابط العضوية المعنية، مثل أطر الزركونيوم المعدنية العضوية. من بين الطرق العديدة المستخدمة لإنشاء أطر الزركونيوم المعدنية العضوية على نطاق النانو، التخليق بمساعدة الموجات الدقيقة، والذوبان الحراري، والسونوكيميائي، والأيونات الحرارية، والميكانيكا الكيميائية. تمت مقارنة تخليق وبنية وتوصيف أطر الزركونيوم المعدنية العضوية في هذا المشروع بين الطرق التقليدية الحرارية والذوبان الحراري والموجات الدقيقة لامتصاص النيتروجين. باستخدام تحليل XRD وFTIR وTGA، تم توصيف العمليتين لتخليق أطر الزركونيوم المعدنية العضوية. توضح النتائج البنية البلورية لكلا الأطر المعدنية العضوية. تتمثل الفوائد الرئيسية للتخليق بمساعدة الموجات الدقيقة مقارنة بالطرق الأخرى في معدل التبلور السريع، ووقت التفاعل القصير، وخصائص أطر الزركونيوم المعدنية العضوية المحسنة. علاوة على ذلك، فإن طريقة مساعدة الميكروويف تعمل على تسريع عملية التركيب بشكل كبير، حيث يتم تحقيق التفاعل الكامل في غضون 10 دقائق عند 120 درجة مئوية، في حين تستغرق العملية التقليدية عادةً 24 ساعة. من النتائج التأسيسية تم الكشف عن أن امتصاص النيتروجين عن طريق التخليق بمساعدة الميكروويف لـ Zr-MOF هو أكثر هيمنة من تقنية التخليق بالفرن التقليدية.

الكلمات المفتاحية: إطار معدني عضوي، المواد المسامية، التخليق بمساعدة الميكروويف، التحضير المذيب الحراري، امتصاص النيتروجين.